2011 50th IEEE Conference on Decision and Control and
European Control Conference (CDC-ECC)
Orlando, FL, USA, December 12-15, 2011

Magnetic Steering of a Distributed Ferrofluid Spot Towards a Deep Target With Minimal Spreading

Arash Komaee and Benjamin Shapiro

Abstract— **In magnetic drug targeting, where drugs are attached to magnetic nanoparticles and external magnets are then used to focus the therapy to, for example, solid tumors, there is a need to better control and focus the distribution of particles (the ferrofluid) to deep targets. This paper considers a key next question: how to move a single spot of ferrofluid to a deep target with minimal spreading. The problem is challenging since the applied magnetic forces have a natural tendency to stretch the ferrofluid spot. A control policy is designed and verified by simulations to optimally control multiple electromagnets in concert to move a single spot of ferrofluid from the edge of a domain to a deep central target with minimal spreading.**

I. Introduction

Magnetic targeting has the potential to enable physical control of medicine to specific locations in the body. In principle, it can enable focusing of chemotherapy to tumors, anticoagulants to blood clots, and antibacterial drugs to infections. Magnetic targeting works by attaching therapy to magnetic nanoparticles, and then using magnets outside the body to direct the therapeutic particles to disease locations [1]–[4]. In the past two decades, such particles have been safely used and magnetic focusing has been demonstrated in animal and phase I human clinical studies [4], [5].

One of the current major limitations in magnetic targeting is design and control of the external magnets to focus particles to deep targets. Prior studies, which used permanent magnets held near surface tumors, have been restricted to shallow targeting depths less than 5 cm [4], [5].

This paper is part of a broad and long term effort in our group to improve the design and control of magnets to better direct magnetized therapy to deep targets. It is known that such deep targeting cannot be achieved without dynamic control – Earnshaw's classic 1842 theorem [6] applies directly to nanoparticles actuated by magnetic fields and proves that no static magnetic field can create an interior stable energy trap. Instead, our group has been focusing on using dynamic control of electromagnets to better drive nanoparticles to deep internal targets. Real-time imaging of magnetic nanoparticles based on fast-MRI technology [7], positron emission tomography (PET) scanning [8], or fast gamma imaging [9] provides a potential means for closed-loop implementation of our control algorithms.

This work was supported by the National Institutes of Health under Grant No. R21EB009265.

A. Komaee is with the Department of Aerospace Engineering, University of Maryland, College Park, MD 20742, USA, e-mail: akomaee@umd.edu.

B. Shapiro is with the Fischell Department of Bio-Engineering and the Institute for Systems Research, University of Maryland, College Park, MD 20742, USA, phone: 301-405-4191, e-mail: benshap@eng.umd.edu.

We have developed experimentally validated simulations of nanoparticle transport *in-vivo* [10], [11], have shown the feasibility of electromagnet control to focus a distributed ferrofluid of nanoparticles to deep targets on average [12], and have demonstrated optimal control of a single drop of ferrofluid in experiments [13]. Now we address the next key question: we ask how to move a spot of ferrofluid from edge to center with minimal spreading. This is still a long way from control of a ferrofluid in animals, or patients, through a vasculature network, under disturbing blood flows, and in the face of large patient-to-patient uncertainty, but it is a substantial next step towards understanding how to effectively control electromagnets to direct magnetic nanoparticles to deep targets.

II. Model and Problem Statement

Consider a flat container filled with a thin layer of a viscous fluid and a distribution of magnetic nanoparticles. The container cross section Ω is a bounded domain in $\mathbb{R}^2$ with the boundary $\partial\Omega$ which prevents the nanoparticles escaping the domain. The concentration $c(r,t)$ of the nanoparticles at any point $r = \begin{bmatrix} r_1 & r_2 \end{bmatrix}^T \in \Omega$ and any time $t \in [0,\infty)$ is defined as the mass of nanoparticles per unit area and is normalized so that

$$\int_\Omega c(r,t)\, dr = 1. \tag{1}$$

The magnetic field inside the domain is generated by n external controlled electromagnets. The resulting magnetic field is described by Maxwell's equations [14]. For an electromagnet with a small time constant and operated in its linear regime [13], [15], the generated magnetic field is proportional to its applied voltage. Let $u_k(t)$ denote the voltage of the k^{th} electromagnet and assume that the vector field $h_k(r) \in \mathbb{R}^2$ characterizes its magnetic field for a unit voltage. The linearity of Maxwell's equations implies that the total magnetic field is given by

$$h(r,t) = \sum_{k=1}^{n} u_k(t)\, h_k(r).$$

This sum can be represented in a matrix form

$$h(r,t) = H(r)\, u(t), \tag{2}$$

where the $n \times 1$ vector $u(t)$ and the $2 \times n$ matrix $H(r)$ are defined as

$$u(t) = \begin{bmatrix} u_1(t) & u_2(t) & \cdots & u_n(t) \end{bmatrix}^T$$
$$H(r) = \begin{bmatrix} h_1(r) & h_2(r) & \cdots & h_n(r) \end{bmatrix}.$$

Throughout the paper, $u(t)$ is regarded as a control vector.

The magnetic force applied to a ferromagnetic particle from a magnetic field $h(r,t)$ is given by

$$f_m(r,t) = k_f \nabla \|h(r,t)\|^2,$$

where $\|\cdot\|$ is the Euclidean norm, the operator ∇ denotes the gradient with respect to r, and $k_f > 0$ is a known constant depending on the volume of the particle and its permeability [1], [16]. Using the matrix representation (2), the magnetic force can be expressed in terms of the control vector $u(t)$ as

$$f_m(r,t) = k_f \nabla \|H(r)\, u(t)\|^2.$$

Note that $\nabla \|H(r)\, u\|^2$ can be explicitly expressed as

$$\nabla \|H(r)\, u\|^2 = \begin{bmatrix} u^T Q_1(r)\, u \\ u^T Q_2(r)\, u \end{bmatrix}, \tag{3}$$

where the $n \times n$ matrices $Q_i(r)$, $i = 1, 2$ are defined as

$$Q_i(r) = \frac{\partial \left(H^T(r)\, H(r)\right)}{\partial r_i}. \tag{4}$$

Since the nanoparticles are surrounded by a viscous fluid, they are subjected to an opposing fluid resistance (drag) in addition to the applied magnetic force. Stokes' drag law states that such a drag force is linear in the velocity of the nanoparticles and is expressed as

$$f_d(r,t) = -\mu v(r,t),$$

where $v(r,t)$ denotes the particle velocity vector at a point r and $\mu > 0$ is a known constant which depends linearly on the diameter of a spherical nanoparticle and the viscosity of the surrounding fluid [16], [17]. The nanoparticle acceleration is negligible since the opposing drag force balances (with an ignorable lag) the magnetic force applied to the particle [16]. Mathematically, this can be stated as $f_m(r,t) + f_d(r,t) = 0$ which is solved for $v(r,t)$ to obtain

$$v(r,t) = \frac{1}{\mu} f_m(r,t).$$

Defining $\alpha = k_f/\mu$ and using the matrix representation of the magnetic force, the velocity vector per particle can be expressed in terms of the control vector $u(t)$ as

$$v(r,t) = \alpha \nabla \|H(r)\, u(t)\|^2. \tag{5}$$

The dynamics of many particles comprising a ferrofluid is derived by considering the nanoparticle flux $\phi(r,t)$ at location r and time t. This flux is comprised of a convection term proportional to the velocity field $v(r,t)$ and a diffusion term proportional to the gradient of the concentration, and is given by

$$\phi(r,t) = -D \nabla c(r,t) + c(r,t)\, v(r,t), \tag{6}$$

where D is a 2×2 matrix of the diffusion coefficients. The concentration rate of change is obtained from the continuity equation [18]

$$\frac{\partial c(r,t)}{\partial t} = -\nabla \cdot \phi(r,t), \tag{7}$$

where $\nabla\cdot$ denotes the divergence operation. Upon substituting (5) and (6) into this equation, the temporal evolution of the concentration can be described by the convection-diffusion partial differential equation (PDE)

$$\frac{\partial c(r,t)}{\partial t} = \nabla \cdot \left(D \nabla c(r,t) - \alpha \nabla \|H(r)\, u(t)\|^2 c(r,t) \right). \tag{8}$$

The boundary condition for this equation must reflect the fact that the nanoparticles cannot leave the domain Ω. To maintain this condition, the flux vector must not have a component perpendicular to the boundary, so the condition

$$i_\Omega(r) \cdot \left(D \nabla c(r,t) - \alpha \nabla \|H(r)\, u(t)\|^2 c(r,t) \right) = 0 \tag{9}$$

must hold over $\partial\Omega$. Here, $i_\Omega(r) \in \mathbb{R}^{2\times 1}$ is the unit vector perpendicular to the boundary at a point r and $\cdot$ denotes the dot product operator.

The partial differential equation (8) describes an infinite-dimensional dynamical system with the concentration $c(r,t)$ as its state and $u(t)$ as its control vector. Although the PDE itself is structurally linear, it represents a nonlinear system due to the quadratic dependence of the magnetic force on the control vector. Given the initial state $c(r,0) = c_0(r)$ and the history of the control vector $u(t)$, the state of the system can be obtained for every arbitrary $t > 0$ by solving this PDE.

A. Problem Statement

Suppose that one of the external electromagnets has been turned on for a long time before $t = 0$, so that at the initial time $t = 0$, the nanoparticles are highly concentrated around a point r_i near the boundary. Denote the initial concentration by $c_0(r)$ and assume that the centroid of this distribution is located at r_i. Let $\mathcal{C}$ be a piecewise differentiable curve in Ω which connects the initial point r_i to a final target r_f. The goal of this paper is to determine a control trajectory $u(t)$ (voltages of the electromagnets) to drive the ferrofluid spot with minimal spreading along $\mathcal{C}$ from r_i to r_f within an unspecified period of time t_f. This must be done despite the natural tendency of magnetic forces to stretch the ferrofluid spot, and it must be achieved in reasonable time and with reasonable control effort.

To develop a mathematical statement for the control problem, we define the mean $\bar{r}(t) \in \mathbb{R}^2$ (center of mass) and the covariance matrix $\Sigma(t) \in \mathbb{R}^{2\times 2}$ of the concentration as

$$\bar{r}(t) = \int_\Omega r c(r,t)\, dr \tag{10}$$

$$\Sigma(t) = \int_\Omega (r - \bar{r}(t))(r - \bar{r}(t))^T c(r,t)\, dr. \tag{11}$$

The trace of the covariance matrix is used as a measure for the size of the ferrofluid spot. To penalize a large final time, one can include a nonnegative increasing function of t_f into the cost function. Thus, the cost function which penalizes both the spot size and the final time can be defined as

$$J = \operatorname{tr}\{\Sigma(t_f)\} + \beta(t_f), \tag{12}$$

where $\beta(\cdot) : [0,\infty) \to [0,\infty)$ is a nonnegative, increasing, and differentiable function satisfying $\beta(0) = 0$.

Based on this cost function, the control problem is: for every $t \in [0, t_f)$, determine a control vector $u(t)$ satisfying $\|u(t)\| \leqslant u_m < \infty$ such that the center of mass $\bar{r}(t)$ moves along the piecewise differentiable curve $\mathcal{C}$ from the initial point r_i towards the final point r_f, and under this control, the cost function (12) attains its minimum.

III. Evolution of Mean and Covariance Matrix

This section provides the preliminary results required in Section IV for the purpose of control design. The procedure of control design is based on a set of equations which determine the derivatives of the mean and the covariance matrix in terms of the concentration $c(r,t)$. These equations are presented in Theorems 1 and 2 below. Lemma 1 provides the necessary background for the proof of these theorems.

Lemma 1: Consider the mapping $w(\cdot) : \mathbb{R}^2 \to \mathbb{R}$ and assume that its partial derivatives exist up to the second order. For every $t > 0$, define the scalar function $\zeta(t)$ as

$$\zeta(t) = \int_\Omega w(r)\, c(r,t)\, dr, \tag{13}$$

where $c(r,t)$ is the solution of the partial differential equation (8) with the boundary condition (9) and the initial condition $c(r,0) = c_0(r)$. Then, the derivative of $\zeta(t)$ is given by

$$\begin{aligned}\dot{\zeta}(t) = &\int_\Omega \nabla w(r) \cdot \alpha \nabla \|H(r)\, u(t)\|^2\, c(r,t)\, dr \\ &+ \int_\Omega \nabla \cdot \left(D^T \nabla w(r)\right) c(r,t)\, dr \\ &- \oint_{\partial\Omega} \nabla w(r) \cdot D\, i_\Omega(r)\, c(r,t)\, d\mathrm{s},\end{aligned} \tag{14}$$

where the last term on the right-hand side is a line integral taken over the boundary $\partial\Omega$.

Proof: Differentiating (13) with respect to t and substituting (7) into the resulting equation, $\dot{\zeta}(t)$ is obtained as

$$\dot{\zeta}(t) = \int_\Omega w(r) \frac{\partial c(r,t)}{\partial t}\, dr = -\int_\Omega w(r)\, \nabla \cdot \phi(r,t)\, dr.$$

Application of the identity

$$w(r)\, \nabla \cdot \phi(r,t) = \nabla \cdot (w(r)\, \phi(r,t)) - \nabla w(r) \cdot \phi(r,t) \tag{15}$$

in the second integral leads to

$$\dot{\zeta}(t) = \int_\Omega \nabla w(r) \cdot \phi(r,t)\, dr - \int_\Omega \nabla \cdot (w(r)\, \phi(r,t))\, dr. \tag{16}$$

Applying the divergence theorem [19] to the second integral and using the boundary condition (9), one can obtain

$$\int_\Omega \nabla \cdot (w(r)\, \phi(r,t))\, dr = \oint_{\partial\Omega} w(r)\, \phi(r,t) \cdot i_\Omega(r)\, d\mathrm{s} = 0.$$

Substituting (5) and (6) into (16), this equation can be expressed as

$$\begin{aligned}\dot{\zeta}(t) = &\int_\Omega \nabla w(r) \cdot \alpha \nabla \|H(r)\, u(t)\|^2\, c(r,t)\, dr \\ &- \int_\Omega \nabla w(r) \cdot D \nabla c(r,t)\, dr.\end{aligned}$$

Using an identity similar to (15), the second integral on the right-hand side of this equation can be written as

$$\begin{aligned}-\int_\Omega \nabla w(r) \cdot D \nabla c(r,t)\, dr \\ = \int_\Omega \nabla \cdot \left(D^T \nabla w(r)\right) c(r,t)\, dr \\ - \int_\Omega \nabla \cdot \left(D^T \nabla w(r)\, c(r,t)\right) dr.\end{aligned}$$

Finally, applying the divergence theorem to the second integral on the right-hand side of this equality leads to the third integral of (14) which completes the proof. ∎

Theorem 1: For every $t > 0$, define the $n \times n$ symmetric matrices $P_i^{\mathrm{m}}(t)$, $i = 1, 2$ (m stands for mean) and the 2×1 vector $b(t)$ as

$$P_i^{\mathrm{m}}(t) = \int_\Omega \alpha Q_i(r)\, c(r,t)\, dr \tag{17}$$

$$b(t) = -\oint_{\partial\Omega} D\, i_\Omega(r)\, c(r,t)\, d\mathrm{s}, \tag{18}$$

where $Q_i(r)$ is given by (4) and $c(r,t)$ is the solution of the partial differential equation (8) with the boundary condition (9) and the initial condition $c(r,0) = c_0(r)$. Then, the derivative of the mean (10) is given by

$$\dot{\bar{r}}(t) = f(u(t), t) + b(t), \tag{19}$$

where $f(\cdot) : \mathbb{R}^n \times \mathbb{R}^+ \to \mathbb{R}^{2\times 1}$ is defined as

$$f(u,t) = \begin{bmatrix} u^T P_1^{\mathrm{m}}(t)\, u \\ u^T P_2^{\mathrm{m}}(t)\, u \end{bmatrix}.$$

Proof: In order to determine the i^{th} element of $\dot{\bar{r}}(t)$, define the mapping $w(r) = e_i \cdot r$, where e_i denotes the i^{th} column of a 2×2 identity matrix. It is easy to show for this mapping that $\nabla w(r) = e_i$ and $\nabla \cdot \left(D^T \nabla w(r)\right) = 0$. Then application of Lemma 1 leads to

$$\begin{aligned}e_i \cdot \dot{\bar{r}}(t) = &\int_\Omega e_i \cdot \alpha \nabla \|H(r)\, u(t)\|^2\, c(r,t)\, dr \\ &- \oint_{\partial\Omega} e_i \cdot D\, i_\Omega(r)\, c(r,t)\, d\mathrm{s}.\end{aligned}$$

Using (3) and considering the definitions (17) and (18), this equation can be expressed as

$$e_i \cdot \dot{\bar{r}}(t) = u^T(t)\, P_i^{\mathrm{m}}(t)\, u(t) + e_i \cdot b(t)$$

which is equation (19) written per element of $\dot{\bar{r}}(t)$. ∎

Theorem 2: Let e_i denote the i^{th} column of a 2×2 identity matrix and define the $n \times n$ matrices $\tilde{P}_{ij}^{\mathrm{c}}(t)$, $i, j = 1, 2$ (c stands for covariance matrix) and the 2×2 matrix $\tilde{B}(t)$ as

$$\tilde{P}_{ij}^{\mathrm{c}}(t) = \int_\Omega e_i \cdot (r - \bar{r}(t))\, \alpha Q_j(r)\, c(r,t)\, dr \tag{20}$$

$$\tilde{B}(t) = D - \oint_{\partial\Omega} (r - \bar{r}(t))\, (D\, i_\Omega(r))^T\, c(r,t)\, d\mathrm{s}, \tag{21}$$

where $c(r,t)$ is the solution of the partial differential equation (8) with the boundary condition (9) and the initial

condition $c(r,0) = c_0(r)$. In terms of these matrices, define the symmetric matrices

$$P_{ij}^{c}(t) = \tilde{P}_{ij}^{c}(t) + \tilde{P}_{ji}^{c}(t) \qquad (22)$$
$$B(t) = \tilde{B}(t) + \tilde{B}^{T}(t).$$

Then, the derivative of the covariance matrix (11) is given by

$$\dot{\Sigma}(t) = F(u(t), t) + B(t), \qquad (23)$$

where $F(\cdot) : \mathbb{R}^n \times \mathbb{R}^+ \to \mathbb{R}^{2\times 2}$ is defined as

$$F(u,t) = \begin{bmatrix} u^T P_{11}^{c}(t)\, u & u^T P_{12}^{c}(t)\, u \\ u^T P_{21}^{c}(t)\, u & u^T P_{22}^{c}(t)\, u \end{bmatrix}. \qquad (24)$$

Proof: Differentiating (11) with respect to t results in

$$\dot{\Sigma}(t) = \frac{d}{dt}\left[\int_{\Omega} (r - \bar{r}(t_0))(r - \bar{r}(t_0))^T c(r,t)\, dr\right]_{t_0=t} - \int_{\Omega} \dot{\bar{r}}(t)(r - \bar{r}(t))^T c(r,t)\, dr - \int_{\Omega} (r - \bar{r}(t))\dot{\bar{r}}^T(t) c(r,t)\, dr.$$

The definition (10) of $\bar{r}(t)$ and the normalizing condition (1) imply that the last two integrals are identically zero. To obtain the ij element of the remaining first integral substitute

$$w(r) = e_i \cdot (r - \bar{r}(t))\, e_j \cdot (r - \bar{r}(t))$$

into (14) of Lemma 1 and note that

$$\nabla w(r) = e_i \cdot (r - \bar{r}(t))\, e_j + e_j \cdot (r - \bar{r}(t))\, e_i$$
$$\nabla \cdot \left(D^T \nabla w(r)\right) = e_i^T \left(D + D^T\right) e_j.$$

By means of this substitution, application of (1) and (3), and the definitions of $P_{ij}^{c}(t)$ and $B(t)$, one can obtain

$$e_i^T \dot{\Sigma}(t)\, e_j = u^T(t) P_{ij}^{c}(t)\, u(t) + e_i^T B(t)\, e_j.$$

The matrix form of this equation is given by (23). ■

IV. Control Design

The phrased control problem does not constrain the final time at which the ferrofluid spot reaches r_f. Since the final time is a variable and must be optimized in the cost function (12), it is convenient to reformulate the problem in terms of arc length, which has a fixed final value. To do so, consider a piecewise differentiable curve $\mathcal{C}$ in Ω which connects the initial point r_i to the final point r_f. Suppose r is an arbitrary point on $\mathcal{C}$ and let s represent the length of the curve segment connecting r_i to r. Denote the total arc length between r_i and r_f by s_f. Assume that $\rho(s)$ is the parametric representation of $\mathcal{C}$ with respect to the arc length s, so that it maps the interval $[0, s_f]$ into the segment of $\mathcal{C}$ between $r_i = \rho(0)$ and $r_f = \rho(s_f)$. As an example, when $\mathcal{C}$ is a straight line extended from r_i to r_f, this representation is given by

$$\rho(s) = r_i + \frac{s(r_f - r_i)}{\|r_f - r_i\|}$$

with $s_f = \|r_f - r_i\|$. An important property of the parametrization $\rho(s)$ is that its derivative $\rho'(s) = d\rho(s)/ds$ has a unit Euclidean norm, i.e., $\|\rho'(s)\| = 1$.

The first objective of the control is to drive the center of mass $\bar{r}(t)$ along $\mathcal{C}$ from r_i to r_f. Since the speed of this point along the curve is a free parameter, there are infinitely many ways to perform this task, and all of them can be described using the parametrization $\rho(s)$. For this purpose, assume that the center of mass departs r_i at $t = 0$, moves along $\mathcal{C}$ with an arbitrary speed $\theta(t) > 0$, and eventually reaches r_f at $t = t_f$, where t_f satisfies the algebraic equation

$$\int_0^{t_f} \theta(\tau)\, d\tau = s_f.$$

Define the strictly increasing map $s(\cdot) : [0, t_f] \to [0, s_f]$ as

$$s(t) = \int_0^t \theta(\tau)\, d\tau. \qquad (25)$$

Then, for some trajectory of $\theta(t)$ and for every $t \in [0, t_f]$, the mean $\bar{r}(t)$ must satisfy

$$\bar{r}(t) = \rho(s(t)), \qquad (26)$$

or equivalently its derivative must satisfy

$$\dot{\bar{r}}(t) = \theta(t)\, \rho'(s(t)).$$

Substituting $\dot{\bar{r}}(t)$ from (19) into this equation leads to the nonlinear algebraic equation

$$f(u(t), t) + b(t) = \theta(t)\, \rho'(s(t)), \qquad (27)$$

which must be satisfied by the the control vector $u(t)$ and the speed $\theta(t)$ for every $t \in [0, t_f)$ in order to maintain (26).

The second objective of the control is to minimize the spread and travel time contained in the cost function (12). To that end, the following lemma expresses this cost function in terms of an integral depending on the trajectories of $u(t)$ and $\theta(t)$ and taken with respect to arc length.

Lemma 2: Let $\theta(\cdot) : [0, \infty) \to (0, \infty)$ be an integrable function and assume that $s = s(t)$ is given by (25). Consider the $n \times n$ matrices $P_{ii}^{c}(t)$, $i = 1, 2$ and the 2×2 matrix $B(t)$ defined in Theorem 2 and for every $t \in [0, \infty)$ define the matrix-valued function

$$W(t) = P_{11}^{c}(t) + P_{22}^{c}(t)$$

and the scalar function

$$\gamma(t) = \operatorname{tr}\{B(t)\} + \dot{\beta}(t).$$

Then, the cost function (12) can be expressed as

$$J = \int_0^{s_f} \frac{u^T(t) W(t) u(t) + \gamma(t)}{\theta(t)}\, ds + \operatorname{tr}\{\Sigma(0)\}, \qquad (28)$$

where $s_f = s(t_f)$ and $u(t) \in \mathbb{R}^n$ is the control vector in (8).

Proof: It is straightforward to show that the cost function (12) can be expressed as

$$J = \int_0^{t_f} \left(\operatorname{tr}\{\dot{\Sigma}(t)\} + \dot{\beta}(t)\right) dt + \operatorname{tr}\{\Sigma(0)\} = \int_0^{s_f} \left(\operatorname{tr}\{\dot{\Sigma}(t)\} + \dot{\beta}(t)\right) \frac{ds}{(ds/dt)} + \operatorname{tr}\{\Sigma(0)\}.$$

Next, substitute $ds/dt = \theta(t)$ from (25) and $\dot{\Sigma}(t)$ from (23) into the second integral to get

$$J = \int_0^{s_f} \frac{\operatorname{tr}\{F(u(t),t) + B(t)\} + \dot{\beta}(t)}{\theta(t)}\, ds + \operatorname{tr}\{\Sigma(0)\}.$$

Considering the quadratic structure of $F(\cdot)$ defined in (24), this integral can be further simplified to (28). ∎

To determine an optimal solution for the control problem, one must perform an optimization over the entire trajectory of the state, using either dynamic programming [20], [21] or Pontryagin's minimum principle [22], [23]. Application of these methods to a general nonlinear problem is difficult, and especially difficult for the present problem due to its infinite-dimensional dynamics. As an alternative, we develop a suboptimal solution for the control problem by a pointwise optimization in the representation (28) of the cost function.

Our approach in resolving the control problem is to minimize the integrand of (28) with respect to $u(t)$ and $\theta(t)$ for every $t \in [0, t_f)$ subject to the equality constraint (27) and the inequality constraints $\|u(t)\| \leqslant u_m$ and $\theta(t) > 0$. Based on this method, the suboptimal control $u^*(t)$ and the suboptimal speed $\theta^*(t)$ are the solution of the constrained optimization problem

$$\begin{aligned} \underset{u,\theta}{\text{minimize}} \;& \frac{u^T W(t)\, u + \gamma(t)}{\theta} \\ \text{subject to}: \;& f(u,t) + b(t) - \theta\rho'(s(t)) = 0, \\ & \|u\| \leqslant u_m, \\ & \theta > 0. \end{aligned} \tag{29}$$

Using the transformation $u = z\sqrt{\theta}$, this optimization problem can be simplified to another optimization problem which has an efficient solution method developed in [13], [15]. To that end, notice that the constraint $\|u\| \leqslant u_m$ holds with equality under the optimal solution, so that $\theta = u_m^2/\|z\|^2$. In addition, the approximation $b(t) \simeq 0$ holds for most of the time during the course of control because the diffusion matrix D is small and, further, the overlap of ferrofluid concentration with the domain boundary $\partial\Omega$ is only appreciable at the very start of the trajectory. Incorporating these two results and exploiting the quadratic structure of $f(\cdot)$, the optimization problem (29) is converted to

$$\begin{aligned} \underset{z}{\text{minimize}} \;& z^T \left(W(t) + u_m^{-2}\gamma(t)\, I_{2\times 2}\right) z \\ \text{subject to}: \;& f(z,t) - \rho'(s(t)) = 0, \end{aligned} \tag{30}$$

where $I_{2\times 2}$ denotes the 2×2 identity matrix. By solving this problem, the optimal values of u and θ in (29) are obtained as

$$\begin{aligned} u^*(t) &= u_m z^*(t) / \|z^*(t)\| \\ \theta^*(t) &= u_m^2 / \|z^*(t)\|^2 \end{aligned}$$

in terms of the solution $z^*(t)$ of (30).

V. Simulation Results

We have evaluated the performance of our proposed control policy by means of a number of computer simulations. In this study, the numerical computations have been performed by an interacting combination of COMSOL Multiphysics® and MATLAB®. The former solves the partial differential equation (8) with the boundary condition (9), and the latter solves the optimization problem (30) using an algorithm developed in [13], [15].

As shown in Fig. 1, the domain Ω in these simulations is a unit circle and $n = 8$ identical electromagnets are equally spaced around this circle. Each individual magnetic field is determined from a model developed in [13] with a magnet length of 4 and magnet diameter of 0.8 (normalized to the radius of Ω). The magnetic fields are normalized such that a unit voltage actuation results in a unit amplitude field at the center of the magnet face.

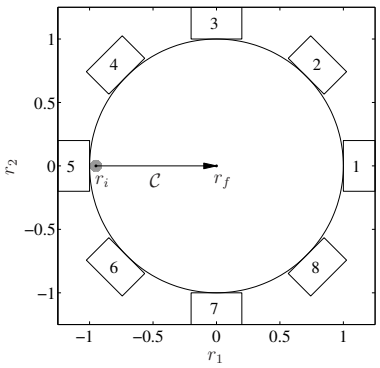

Fig. 1. The geometry used for the simulations. The small rectangles marked with 1 through 8 represent the electromagnets. The straight line extended from r_i towards r_f is the trajectory of the spot of ferrofluid. The initial concentration of ferrofluid $c_0(r)$ is shown in light gray.

The parameters used in the simulations are $\alpha = 1$, $u_m = 1$, and $D = 10^{-5} I_{2\times 2}$. The scalar function $\beta(\cdot)$ in (12) is assumed to be $\beta(t) = 9 \times 10^{-5}\, t$. The initial concentration $c_0(r)$ is uniform over a circle of radius 0.05 which is centered at the initial point $r_i = [-0.95 \quad 0]^T$, while the final point r_f is the origin of coordinate system. Finally, the curve $\mathcal{C}$ is a straight line connecting r_i to r_f.

The simulation results are presented in Fig. 2 and Fig. 3. Fig. 2 illustrates the concentration $c(r,t)$ as the spot is moved from left to right. In this figure, two control policies are compared: the right column shows the concentration under the proposed control, while the left column presents the concentration under a trivial control in which electromagnet 1 is energized with its maximum power and the rest of electromagnets are turned off. Fig. 3 shows the trace of the covariance matrix as the ferrofluid spot is controlled from left to right by the optimal (solid line) and trivial (dashed) electromagnet control. This plot indicates that the optimal control confines the droplet 8 times better by the time it reaches the central target point.

VI. Conclusion

The motion of a spot of distributed ferrofluid under a controlled magnetic field has been described by a convection-diffusion partial differential equation. Based on this model, a control policy has been developed to steer the ferrofluid spot along an arbitrary trajectory from an initial point towards a

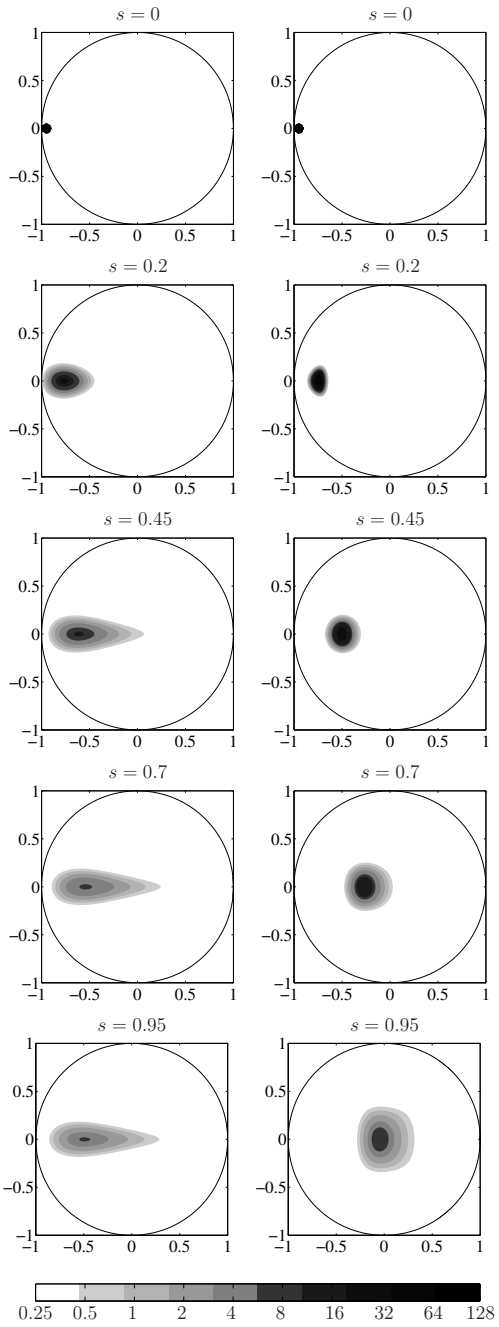

Fig. 2. Concentration profile at $s = 0, 0.2, 0.45, 0.7, 0.95$. The right column shows the concentration under the proposed control, while the left column presents the concentration under a trivial control in which electromagnet 1 is energized with its maximum power and the rest of the electromagnets are turned off.

desired final point. The control has been designed to maintain the spot size at the final point as small as possible. Numerical simulations have been performed to verify the performance of the proposed control policy.

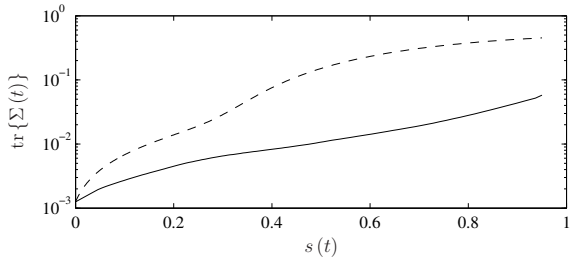

Fig. 3. Trace of the covariance matrices versus arc length, for the proposed control (solid line), and for the trivial control (dashed line).

REFERENCES

[1] Q. A. Pankhurst, J. Connolly, S. K. Jones, and J. Dobson, "Applications of magnetic nanoparticles in biomedicine," *J. Phys. D: Appl. Phys.*, vol. 36, pp. R167–R181, Jun. 2003.

[2] M. Arrueboa, R. Fernández-Pachecoa, M. R. Ibarraa, and J. Santamaría, "Magnetic nanoparticles for drug delivery," *Nano Today*, vol. 2, pp. 22–32, Jun. 2007.

[3] N. M. Orekhova, R. S. Akchurin, A. A. Belyaevand, M. D. Smirnov, S. E. Ragimov, and A. N. Orekhov, "Local prevention of trombosis in animal arteries by means of magnetic targeting of aspirin-loaded red cells," *Thrombosis Research*, vol. 57, pp. 611–616, Feb. 1990.

[4] A. S. Lübbe, C. Alexiou, and C. Bergemann, "Clinical applications of magnetic drug targeting," *Journal of Surgical Research*, vol. 95, no. 2, pp. 200–206, 2001.

[5] A. J. Lemke, M. I. Senfft von Pilsach, A. Lübbe, C. Bergemann, H. Riess, and R. Felix, "MRI after magnetic drug targeting in patients with advanced solid malignant tumors," *European Radiology*, vol. 14, no. 11, pp. 1949–1955, 2004.

[6] S. Earnshaw, "On the nature of the molecular forces which regulate the constitution of the luminiferous ether," *Trans. Camb. Phil. Soc.*, vol. 7, pp. 97–112, 1842.

[7] S. Fricke, I. N. Weinberg, P. Stepanov, S. Glidden, A. McMillan, and P. M. Starewicz, "Threshold for peripheral nerve stimulation with ultra-fast gradients," in *Proc. of the 19th Meeting of the Society for Magnetic Resonance in Medicine*, Montreal 2011.

[8] N. K. Devaraj, E. J. Keliher, G. M. Thurber, M. Nahrendorf, and R. Weissleder, "18F labeled nanoparticles for in vivo PET-CT imaging," *Bioconjugate Chem.*, vol. 20, pp. 397–401, Jan. 2009.

[9] S. I. Parker, C. J. Kenney, D. Gnani, A. C. Thompson, E. Mandelli, G. Meddeler, J. Hasi, J. Morse, and E. M. Westbrook, "3DX: an X-ray pixel array detector with active edges," *IEEE Trans. Nucl. Sci.*, vol. 53, pp. 1676–1688, Jun. 2006.

[10] A. Nacev, C. Beni, O. Bruno, and B. Shapiro, "Magnetic nanoparticle transport within flowing blood and into surrounding tissue," *Nanomedicine*, vol. 5, pp. 1459–1466, Nov. 2010.

[11] A. Nacev, C. Beni, O. Bruno, and B. Shapiro, "The behaviors of ferromagnetic nano-particles in and around blood vessels under applied magnetic fields," *Journal of Magnetism and Magnetic Materials*, vol. 323, pp. 651–668, Mar. 2011.

[12] B. Shapiro, "Towards dynamic control of magnetic fields to focus magnetic carriers to targets deep inside the body," *Journal of Magnetism and Magnetic Materials*, vol. 321, pp. 1594–1599, May 2009.

[13] A. Komaee and B. Shapiro, "Steering a ferromagnetic particle by optimal magnetic feedback control," *IEEE Trans. Contr. Syst. Technol.*, 2011.

[14] R. P. Feynman, R. B. Leighton, and M. Sands, *The Feynman Lectures on Physics*. San Francisco: Pearson/Addison-Wesley, 2006.

[15] A. Komaee and B. Shapiro, "Steering a ferromagnetic particle by magnetic feedback control: Algorithm design and validation," in *Proc. of the 2010 American Control Conference*, pp. 6543–6548, Jun. 30 – Jul. 2 2010.

[16] C. I. Mikkelsen, *Magnetic Separation and Hydrodynamic Interactions in Microfluidic Systems*. PhD thesis, Technical University of Denmark, 2005.

[17] R. F. Probstein, *Physicochemical Hydrodynamics: An Introduction*. New York: John Wiley & Sons, 2nd ed., 1994.

[18] L. D. Landau and E. M. Lifshitz, *Fluid Mechanics*. Oxford, England: Pergamon Press, 2nd ed., 1987.

[19] T. M. Apostol, *Calculus*, vol. 2. New York: Wiley, 2nd ed., 1967 - 1969.

[20] R. Bellman, *Dynamic Programming*. Princeton: Princeton University Press, 1962.

[21] D. P. Bertsekas, *Dynamic Programming and Optimal Control*. Belmont, MA: Athena Scientific, 3rd ed., 2005.

[22] D. E. Kirk, *Optimal Control Theory: an Introduction*. Englewood Cliffs, NJ: Prentice-Hall, 1970.

[23] M. Athans and P. L. Falb, *Optimal Control : an Introduction to the Theory and Its Applications*. New York: McGraw-Hill, 1966.